Deformation and Failure of Polymeric Matrices under Swelling Conditions*

DANIEL COHN † and GAD MAROM, *Casali Institute of Applied Chemistry, School of Applied Science and Technology, The Hebrew University of Jerusalem, 91904 Jerusalem, Israel*

Synopsis

Polymers in which the diffusion mechanism was characterized by a sharp advancing boundary between the swollen shell and the core showed a highly anisotropic swelling response. The anisotropy of the swelling strains was caused by the mechanical constraints exerted mutually by the two regions of the specimen. The swelling stresses developing during the process eventually led to fracture of the polymer specimen. An analytical model which explained the modes of failure of the polymer under the swelling stresses was developed. The proposed approach was based on the general analogy existing between the studied swollen specimens and composite materials. A model for the prediction of the anisotropic hygroelastic response of the swollen systems was also proposed.

INTRODUCTION

The two fundamental issues which determine the performance of a polymer in service conditions which expose it to a liquid environment are its dimensional stability and mechanical integrity. The topic of hygroelasticity, defined as the reversible dimensional response of a polymer resulting from liquid penetration, has been the subject of our studies for a number of years now.[1–5] Our early studies were confined to polymer–liquid systems which exhibited a Fickian behavior; lately we focused on Case II systems, in which the diffusion mechanism is characterized by a sharp advancing front, separating the inner glassy core from the swollen shell. This feature, as shown below, dictates the dimensional response and modes of failure of the swollen polymer. A detailed account of the hygroelastic behavior of PMMA swollen by methanol was recently given.[6] The results of that study revealed a clearly anisotropic response, the extent of which depended on the geometry of the specimen. It was pointed out that since the anisotropy of the swelling strains was caused by the mechanical constraints exerted by the core on the shell, the dimensions of the interfaces across which these constraints were transferred were of primary importance. Specifically, the size and relative dimensions of the core were essential in determining the anisotropic response of the polymer in a Case II diffusion. Finally, light was shed on the mechanism of the appearance of tensile and shear stresses between the swollen expanding envelope and the glassy stiff core.

A number of features exhibited by the PMMA system investigated were seen

* Presented at the 37th Annual Conference, Reinforced Plastics/Composite Institute, SPI, Inc., January, 1982, Washington, D.C.

† Present address: Benson Hall, Dept. of Chemical Engineering, University of Washington, Seattle, WA 98195.

Journal of Applied Polymer Science, Vol. 28, 1981–1992 (1983)
 CCC 0021-8995/83/061981-12$02.20

as a direct consequence of the fact that PMMA is a thermoplastic uncrosslinked polymer, in which the occurrence of plastic flow phenomena could cause both irreversible deformations and stress relaxation processes.[6] Previous findings also showed the importance of several morphological factors (e.g., the free volume of the polymer, molecular orientation or crosslink density) in determining the hygroelastic response of a polymeric matrix.[7] In the light of these considerations, it was important to study the behavior of a thermosetting polymer, in which the intermolecular covalent crosslink bonds were expected to prevent the occurrence of plastic flow phenomena. Consequently, an epoxy resin was investigated, and the results are presented in this paper.

Since the use of polymers often entails contacts with liquid environments, their dimensional stability and long-term mechanical stability turn to be limiting factors. In view of this, and in conjunction with our experimental data, analytical tools were developed, which enabled us to predict both the hygroelastic response of the polymer and its modes of failure. The analysis was based on a shell-core stress transfer model.

EXPERIMENTAL

The experimental work was carried out with the following resin–liquid system: epoxy resin (Araldite MY 750/HT 972)–methylene chloride. The specimens, having various geometries, were taken out periodically for weighing and dilatation measurements. The recordings were carried out at 23°C and each specimen was cooled down in methylene chloride before readings were taken. ΔL was measured by placing each specimen in a stainless steel fixture attached to a dial gauge capable of measuring to half a micron. The maximum temperature variation allowed during ΔL measurements was ± 0.5°C, and this resulted in ΔL change of less than about 1 μm.

The dimensional changes due to the solvent penetration were measured for each specimen along the three axes, x, y, and z (width, length, and thickness, respectively). The three relative dimensional changes were then plotted against $\Delta V^*/V_0$ and the corresponding coefficients of hygroelasticity, μ_x, μ_y, and μ_z were worked out from the initial slope of the resulting curves. In order to follow the advancing front, thin slices were cut along the specimen different axes, and front penetration measurements were performed using an eyepiece micrometer. Photoelastic techniques were used as well.

RESULTS AND DISCUSSION

Figure 1 presents the swelling data of an epoxy specimen ($10.0 \times 1.9 \times 0.9$ cm^3) in methylene chloride, as expressed by the relative dimensional changes along the x, y, and z directions during the liquid immersion period. By plotting the swelling strains vs. the solvent takeup as expressed by $\Delta V^*/V_0$, the directional coefficients of hygroelasticity are derived. The overall response pattern exhibited by the different specimens studied is generally similar, indicating that variations in the specimen geometry affect the behavior only quantitatively. Thus, the data presented in Figure 1 are viewed as exemplifying the essential features of the hygroelastic response of the polymer under the swelling conditions investigated.

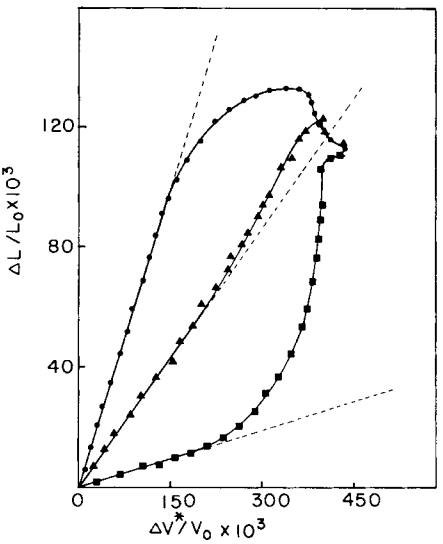

Fig. 1. Plots of the swelling strains vs. $\Delta V^*/V_0$ for an epoxy specimen ($10.0 \times 1.9 \times 0.9$ cm^3) immersed in methylene chloride at 35°C: (▲) x-axis; (■) y-axis; (●) z-axis.

The complex hygroelastic behavior obtained was characterized by the following elements: (a) A first period during which the system showed a highly anisotropic dimensional response, with very small swelling strains along the long axes of the specimen and very large strains along the specimen thickness; (b) with the continuation of the process, a drastic change in the hygroelastic behavior occurred, resulting in a rearrangement of the specimen strains; at this point, an abrupt shrinkage along the z-axis was observed, with a concomitant large expansion along the other two directions; and (c) an isotropic behavior, with equal directional strains along the three axes was observed after the sharp transition.

A previous work[1] showed that the upper bound for the coefficient of hygroelasticity in an isotropic system is 0.33. Yet, the data plotted in Figure 1 yields the three directional coefficients of $\mu_x = 0.290$, $\mu_y = 0.064$, and $\mu_z = 0.670$. The anisotropy of the system is obvious, and it is important to note that μ_z is significantly larger than the upper bound found for μ in isotropic systems.

In our work[6] on the PMMA–methanol swelling system, two specific features of the overall behavior encountered were seen as a direct consequence of the fact that PMMA was a thermoplastic noncrosslinked polymer: (i) The final swelling strains along the x- and y-axes (width and length, respectively) were identical, whereas across the thickness (z-axis) somewhat larger strains were observed. This was attributed to the fact that along the z-axis plastic deformation, in addition to the swelling strains, took place. It was suggested that the excessively high strains along the z-axis were induced by a "squeezing-out" effect. (ii) Flow processes also led to a partial relaxation of the shear stresses developed at the boundary between the shell and the core. This relaxation seriously limited the buildup of stresses in the core and, therefore, prevented failure of the numerous PMMA specimens studied.

As opposed to the PMMA systems, it is apparent (Fig. 1) that in the epoxy systems a final isotropic response is obtained. This is attributed to the fact that

the strong intermolecular crosslink bonds prevent the occurrence of any significant plastic flow along the z-axis.

The second phenomenon exhibited exclusively by the crosslinked resins is the macroscopic cracking of the swollen sample. This is attributed to the fact that the tensile and shear stresses, imposed by the swollen expanding shell on the core through the interfacial surface, eventually lead to failure. Figure 2 shows an epoxy sample ($5.0 \times 3.0 \times 0.5$ cm^3) swollen by methylene chloride at the beginning of the failure process, with the appearance of the first crack and as the cracking proceeds. Two types of cracks are evident: boundary cracks, formed at the advancing boundary (see Fig. 3) and core cracks, formed within the brittle core (see Fig. 4). It is important to note that all cracks are in the xz plane, resulting in a symmetrical array along the y axis. This is evident from Figures 2 and 5, where a fractured sample is shown, using photoelastic techniques. Eventually, the dimensional constraint imposed by the core on the swollen shell is relaxed when a crack is formed as seen in Figure 6.

A SHELL-CORE STRESS TRANSFER MODEL

It is well known that liquid molecules significantly affect the properties of the penetrated polymer,[8–10] special attention being given to the plasticizing effect of the solvent, which results in a sharp decrease in Young's modulus.[11,12] It is, therefore, clear that the mechanical properties of the two distinct regions of the specimen will be very different. On these grounds, such a swelling system is

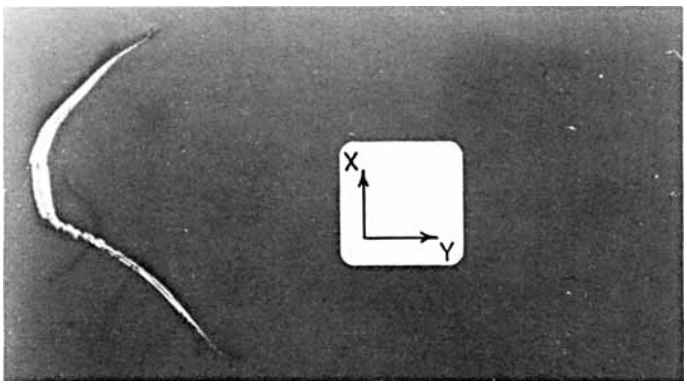

(a)

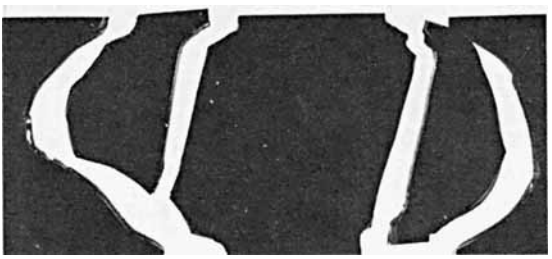

(b)

Fig. 2. An epoxy specimen ($5.0 \times 3.0 \times 0.5$ cm^3) showing the first boundary crack (a) and the final symmetrical array of boundary and core cracks (b).

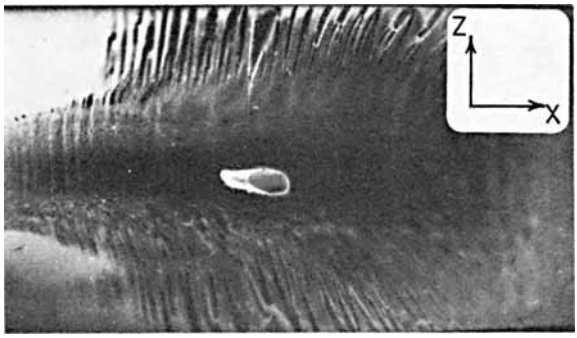

Fig. 3. A view of the crack surface of a boundary crack.

viewed in this study as analogous to a composite material comprising a stiff "fiber" embedded in a soft matrix.

An analytical model which explains the modes of failure and the symmetrical arrangement of the cracks in the specimens is presented. Only two assumptions are made: (a) The core has a truncated ellipsoid shape, having an elliptical cross section, and (b) the maximum shear stress is obtained at the edge of the core along the y-axis and then decreases toward the center. During the early stages of the swelling process, the general shape of the core is essentially that of the specimen, but, as the penetration along the three axes proceeds, the core obtains an elliptical geometry, as can be clearly seen in Figures 7 and 8. The precise manner in which the stresses in fiber-reinforced polymers vary has been obtained analytically for a number of model situations. In spite of the fact that different assumptions have been made concerning the variation of the shear stress at the fiber–matrix interface along the longitudinal axis, there is a general agreement that the shear stress is maximum at the fiber edge and that it diminishes toward the center.[13–15] Similarily, in our system, we look at the behavior of an infinitesimal swelling element adjacent to the interface, and take into account the additivity of the restraint imposed by the core on the deformation of consecutive swelling elements. It is clear that the maximum shear stress is obtained at the edge of the core. Since it is apparent that the higher tensile stresses in the core will develop along the y direction, these will represent the extreme conditions of the system, and the proposed model is examined in this paper, only along the y-axis.

The model refers to a sample having, at a given time t, the following dimen-

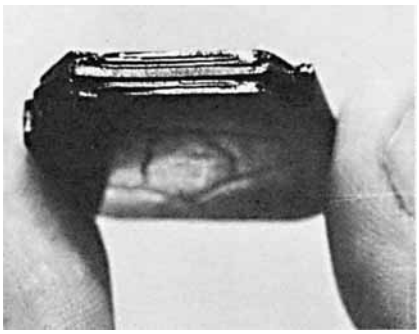

Fig. 4. A general view of a core crack.

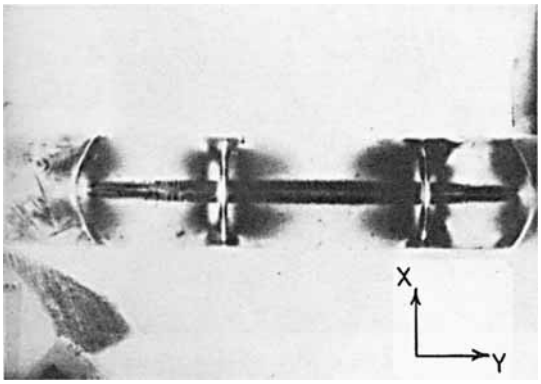

Fig. 5. A swollen specimen between polaroids showing the development of two boundary and two core cracks arranged symmetrically with respect to the midplane of the specimen.

sions: X_0, Y_0, and Z_0. X, Y, and Z are the three axes of the ellipsoid from which the truncated one was derived. Since a 20% truncation was assumed (on the basis of numerous experimental observations), the actual dimensions of the core are $X, 0.8Y, Z$. The shear stress at the boundary is

$$\tau(y^*) = \tau_{\max} - By^* \tag{1}$$

where y^* is the distance from the edge of the core along the y-axis, B is a constant, and $\tau(y^*)$ is the shear stress at the interfacial surface. The stress distribution along the length of the core is understood by considering the equilibrium of a small element of the core, as follows:

$$A(y^*)\sigma(y^*) + \tau(y^*)P(y^*)dy^* = [A(y^*) + dA][\sigma(y^*) + d\sigma] \tag{2}$$

where $A(y^*)$ is the cross-sectional area of the core, $P(y^*)$ is the perimeter of the core, and $\sigma(y^*)$ is the tensile stress in the core (see Fig. 9). Note the analogy to the stress transfer mechanism considered in the analysis of the fiber critical length in fiber-reinforced composites.[13]

On the basis of the assumptions made, very simple geometrical considerations[16,17] led to expressions for $A(y^*)$ and $P(y^*)$. Once $A(y^*)$ was differentiated

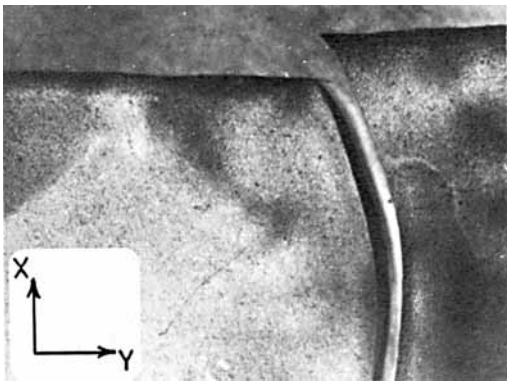

Fig. 6. The dimensional constraint imposed by the core on the swollen shell is relaxed when a crack is formed.

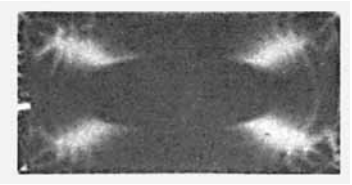

Fig. 7. A view at right angle to xy plane of a specimen placed between polaroids, showing the ellipsoid shape of the core.

with respect to y^*, the above differential equation was solved, and an expression based on the varying geometrical parameters of the core was obtained:

$$\sigma(y^*) = \frac{\sqrt{2}\,Y(X^2+Z^2)^{1/2}}{XZW}\Big\{(W)^{1/2}\{(0.5y^* - 0.2Y)\tau_{\max} - B[0.1Y(2y^* - 0.8Y) - 0.33W]\} + Y^2\left[\arcsin\left(\frac{-2y^* + 0.8Y}{Y}\right)\right](0.05YB - 0.13\tau_{\max}) + C(0)\Big\} \quad (3)$$

where $W = -y^{*2} + 0.8y^* + 0.9Y^2$. It describes the variation of the tensile stress along the core, as a function of the distance y^* from its edge.

This model was examined with six different specimens swollen by methylene chloride at 35°C, and the experimental results were in close agreement with the theoretical predictions. Figure 10 is a graphical presentation of the tensile stress in the core, as a function of the distance from its edge, for an epoxy specimen (10.0 × 1.9 × 0.9 cm^3), as obtained by eq. (3). The mechanical data required for this equation were determined experimentally, or values taken from the literature were used.

It is important to note that the general form of the $\sigma(y^*)$ function shows a rapid rise in the tensile stress until a maximum ($\sigma_{\max}$) is achieved and a subsequent drop from that point toward the middle of the core.

Experimentally, the first core crack appeared after 970 h of swelling, at a distance of 1.2 cm from the edge. The maximum core stress and the coordinate of its location as a function of the swelling time, are presented graphically in Figure 11. Cracking will occur whenever $(\sigma_{\text{core}})_{\max} = \sigma_F$, where σ_F is the fracture stress of the dry polymer. Since the tensile strength of the dry epoxy resin is

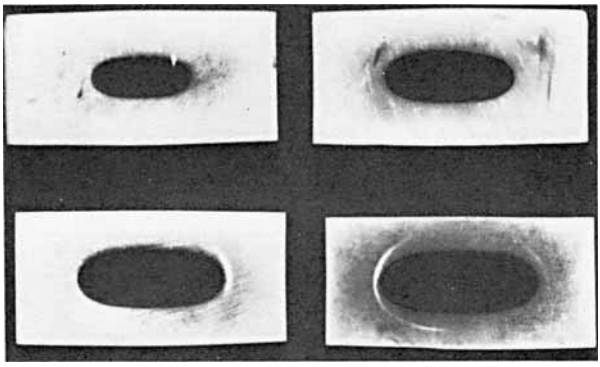

Fig. 8. Cross-sections through the xz plane of an epoxy specimen as swelling proceeds.

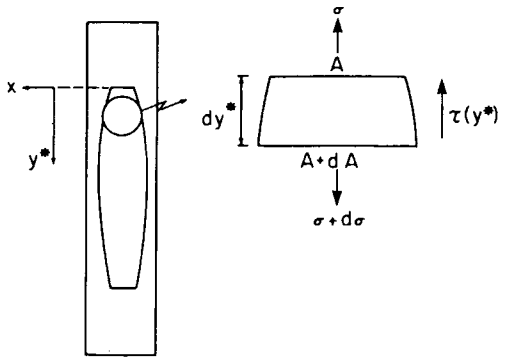

Fig. 9. A two-dimensional schematic description of a partially swollen specimen.

in the range of 80–85 MPa, it is seen that our experimental findings are in very good agreement with our theoretical predictions.

As the swelling prceeds, the sharp boundary advances steadily and the size of the core reduces. Consequently, the surface to volume ratio of the core increases, or in a simpler two-dimensional approach, the cross-section ratio P/A increases.

Figure 12 shows a plot of the perimeter to cross-sectional area ratio (P/A) vs. the swelling time. It can be seen that the proportions of the core undergo, at a particular moment (for this specimen after 930 h), a sharp transition. The P/A ratio is directly related to the efficiency of stress transfer mechanism acting

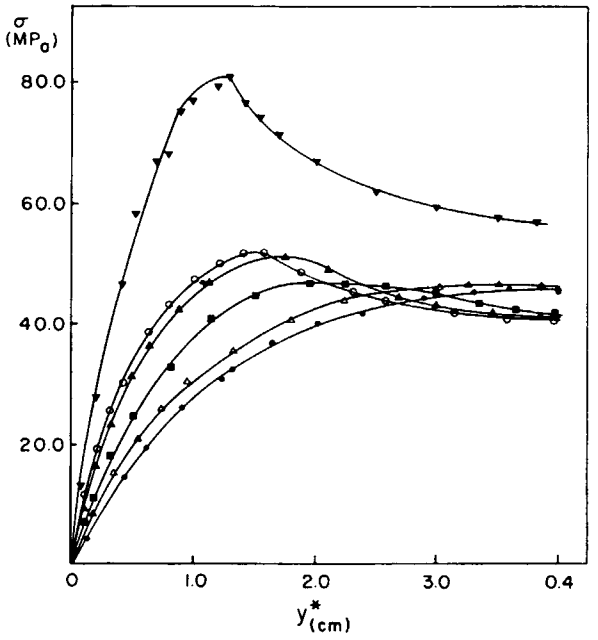

Fig. 10. The tensile stresses in the core as a function of the distance from its edge for an epoxy specimen (of Fig. 1) as obtained by eq. (3) for different swelling periods (h): (●) 100; (△) 250; (■) 550; (▲) 750; (●) 850; (▼) 960.

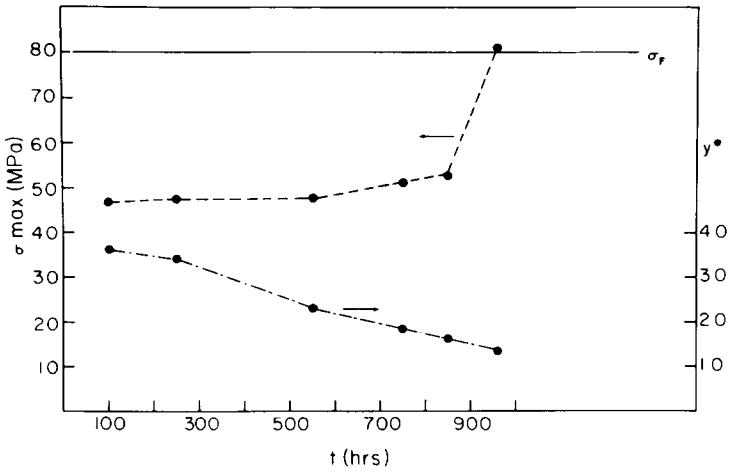

Fig. 11. The maximum core stress and the coordinate of its location as a function of the swelling time (specimen of Fig. 1).

between the swollen shell and the core. The shear stresses at the interface are transferred to the core, building up tensile stresses in it. As a result, the bigger the P/A ratio is, the higher the tensile stress in the core at a given distance from its edge. It is important to note that the drastic increase in the tensile stresses at the core seen in Figures 10 and 11, leading ultimately to its fracture, occurs simultaneously with the sharp growth in the P/A ratio (see Fig. 12) bringing the core to a critical failure geometry. This emphasizes, once again, the primary

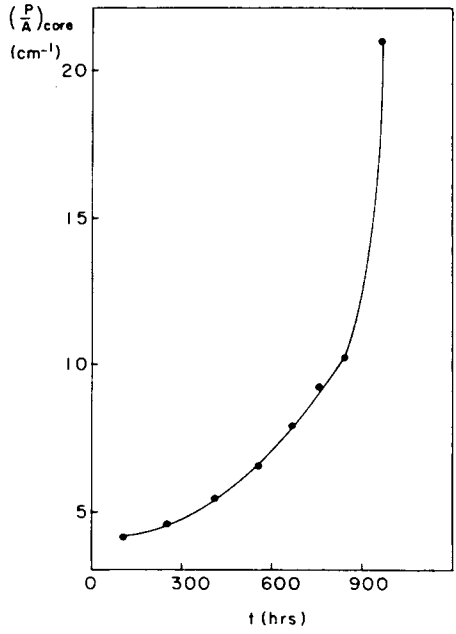

Fig. 12. A plot of the perimeter to cross-sectional area ratio (P/A) vs. the swelling time (specimen of Fig. 1).

importance of the geometrical parameters in determining whether or not the specimen will undergo cracking.

The formation of the cracks in the xz plane along the long axis, y, and their symmetrical arrangement (Fig. 13) are also explained by the proposed model. The first is a direct consequence of the fact that higher shear stresses develop along the longest axis, and the second is a result of the symmetry of the problem, whereby σ_{max} are located symmetrically at the same distance from both core edges. Thus, it is possible to predict if and when a specimen will fail, based on the specimen geometry, and using the theoretical model proposed and the general kinetics of the diffusion process.

ANISOTROPIC HYGROELASTICITY

In the last phase of this study a model for the prediction of the anisotropic hygroelastic response of swollen specimens, based on the directional coefficients of hygroelasticity was developed.

Since the anisotropy of the swelling strains is caused by the mechanical constraints exerted mutually by the two regions of the specimen, the size and dimensions of the interfacial surface are essential in determining the anisotropic response of the sample. In the light of these considerations, the analytical tools proposed were based on the relation existing between the anisotropy of the hygroelastic behavior of the polymer and the deviation of the specimen geometry from a cube. It is clear that the extent of the restraint along a certain axis will be a function of both the absolute and relative dimensions of the core in that given direction. It is also apparent that a cubic sample will show an isotropic hygroelastic behavior. Since the anisotropy of the hygroelastic response of the polymer is directly linked to its geometry, the proposed analysis considers the ratios of the initial dimensions of the specimen and those of a cube with an identical surface area, regarded as an "equivalent cube."

The proposed model regards the geometry of the specimen as being that of the core at time zero. In addition, it assumes that as the swelling proceeds the core will maintain the original relative dimensions of the specimen. This will

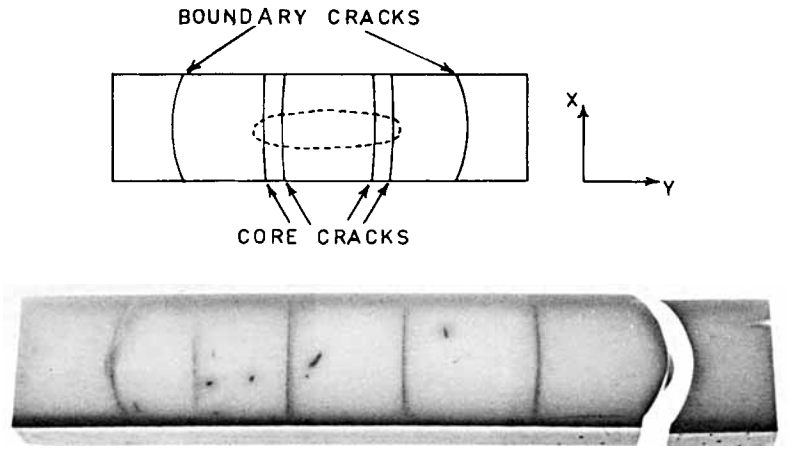

Fig. 13. An epoxy specimen after a prolonged exposure to methylene chloride (specimen of Fig. 1); the diagram identifies boundary and core cracks.

be so until the core geometry, and more specifically its P/A ratio, will undergo a sharp change, coinciding with the limit of the applicability of the proposed model. The anisotropic dimensional response is studied in terms of directional coefficients of hygroelasticity, μ_i ($i = x, y, z$). The three equal directional coefficients of a cubic specimen, μ_i, are expressed by $\bar{\mu}$. The bulk coefficient of hygroelasticity, μ_v, is defined as follows:

$$\mu_v = \sum_i \mu_i \quad (i = x, y, z) \tag{4}$$

The dimensions of the specimen are taken as X, Y, and Z. Since the deviation of the specimen geometry from a cube plays a decisive role, deviation ratios Q_J are defined as the ratios between the side length (L) of the "equivalent cube" (having the same total surface area as the specimen) and the length of each of the specimen axes J ($J = X, Y, Z$). Due to the mechanism by which the mechanical constraint imposed by the core is transferred to the swollen envelope, a linear relationship is assumed between the extent of deviation from a cubic geometry along a given axis and the directional coefficients of hygroelasticity.

On this basis, a simple expression for the directional coefficients of hygroelasticity was developed:

$$\mu_i = \frac{\mu_v}{J\Sigma(1/J)} \quad (i = x, y, z, J = X, Y, Z) \tag{5}$$

The most general definition of the coefficient of hygroelasticity is[1]

$$\mu = \frac{\Delta L/L_0}{\Delta V^*/V_0} \tag{6}$$

where $\Delta L/L_0$ is the relative length change, ΔV^* is the volume of the penetrating liquid, and V_0 is the initial volume of the polymer. Let ΔV denote the volume change of the polymer, due to diffusion of a volume of liquid ΔV^*. Therefore, $\Delta V^* = \Delta V + \delta$, where δ accounts for the volume of the liquid molecules which occupy a fraction of the free volume of the polymer, without causing any volume increase. The upper bound for the volume increase of the polymer, due to liquid diffusion is reached when $\delta = 0$, resulting in $\mu = 0.33$. Since the swelling system under study is characterized by a sharp advancing front, it is clear that the segmental relaxation processes are slower than the penetrant mobility. Under these circumstances, it is reasonable to assume that δ is negligible. Hence, $\mu_v = 1.00$ and eq. (5) reduces to the simpler equation

$$\mu_i = \frac{1}{J\Sigma(1/J)} \tag{7}$$

Equation (7) was tested using six different specimens and the experimental results, shown in Table I, were found to be in excellent agreement with the theoretical predictions. The fact that the experimental values of μ_v are approximately equal to 1.00 strongly supports the assumption that δ is negligible for this system. Moreover, it is important to note that the more the geometry of the specimen deviates from a cubic one, the larger the anisotropy of the dimensional response, as predicted. The longitudinal restraint increases, implying smaller μ_y values, as the length of the specimen increases, and the swelling strains along the z-axis are higher for thinner specimens. All these features are in complete accordance with the theoretical basis of the proposed model.

TABLE I
Theoretical and Experimental Directional Ceofficients of Hygroelasticity for Different Epoxy Specimens Swollen by Methylene Chloride at 35°C

μ_v	μ_z		μ_x		μ_y		Specimen
Exptl.	Theoret.	Exptl.	Theoret.	Exptl.	Theoret.	Exptl.	geometry (cm^3)
1.024	0.665	0.670	0.299	0.290	0.060	0.064	10.0 × 1.9 × 0.9
0.992	0.798	0.782	0.161	0.170	0.032	0.040	10.0 × 1.9 × 0.4
0.964	0.861	0.845	0.086	0.097	0.017	0.022	10.0 × 1.9 × 0.2
0.997	0.600	0.583	0.268	0.266	0.134	0.148	4.0 × 1.9 × 0.9
1.000	0.769	0.762	0.154	0.147	0.077	0.091	4.0 × 1.9 × 0.4
0.959	0.834	0.820	0.083	0.089	0.042	0.048	4.0 × 1.9 × 0.2

CONCLUSIONS

The main conclusions of the present study are summarized as follows:

(1) Swelling systems in which the diffusion mechanism is characterized by an advancing front show an anisotropic hygroelastic behavior.

(2) The size of the core and its relative dimensions determine the directional swelling strains of the polymer sample.

(3) The crosslinked nature of the swollen matrix is an important morphological factor, significantly affecting both the swelling strains and especially the stresses developed in the system.

(4) The cracking under swelling stresses is explained in terms of the general analogy between the swollen systems and fiber-reinforced composite materials. On this basis, a stress transfer model is developed and successfully tested.

(5) A simple expression for the directional coefficients of hygroelasticity, based on the initial geometry of the specimen, is proposed, and is in very good agreement with the experimental results.

References

1. D. Cohn and G. Marom, *Polym. Eng. Sci.*, **18**, 1001 (1978).
2. D. Cohn and G. Marom, *Polymer*, **20**, 501 (1979).
3. D. Cohn and G. Marom, *Polymer*, **24**, 223 (1983).
4. G. Marom, *Polym. Eng. Sci.*, **17**, 799 (1977).
5. G. Marom and D. Cohn, *J. Mater. Sci.*, **15**, 631 (1980).
6. D. Cohn and G. Marom, *Polym. Eng. Sci.*, **22**, 870 (1982).
7. D. Cohn, Ph.D. thesis, The Hebrew University, Jerusalem, 1981.
8. P. J. Flory, *J. Am. Chem. Soc.*, **67**, 2048 (1945).
9. A. S. Ribnick, H. D. Weigmann, and L. Rebenfeld, *Text. Res. J.*, **42**, 720 (1972).
10. H. D. Weigmann and A. S. Ribnick, *Text. Res. J.*, **44**, 165 (1974).
11. M. Gordon and J. S. Taylor, *J. Appl. Chem.*, **2**, 493 (1952).
12. M. C. Shen and A. V. Tobolsky, *Adv. Chem. Ser.*, **48**, 118 (1965).
13. B. D. Agarwal and L. J. Broutman, *Analysis and Performance of Fiber Composites*, Wiley, New York, 1980.
14. W. R. Tyson and G. J. Davies, *Brit. J. Appl. Phys.*, **16**, 199 (1965).
15. J. G. Morley, *Chem. Brit.*, **10**(12), 478 (1974).
16. *Standard Mathematical Tables*, 20th ed., CRC Press, (1972).
17. M. Sadosky and R. Guber, *Elementos de Calculo Diferencial e Integral*, Libreria y Edirotial Alsina, Buenos Aires, 1965.

Received August 30, 1982
Accepted January 18, 1983